

# M1- and M2-macrophage polarization in thioacetamide (TAA)-induced rat liver lesions; a possible analysis for hepato-pathology

**Kavindra Kumara Wijesundera, Takeshi Izawa, Hiroshi Murakami, Anusha Hemamali Tennakoon, Hossain M. Golbar, Chisa Katou-Ichikawa, Miyuu Tanaka, Mitsuru Kuwamura and Jyoji Yamate**

Laboratory of Veterinary Pathology, Division of Veterinary Sciences, Graduate School of Life and Environmental Sciences, Osaka Prefecture University, Izumisano city, Osaka, Japan

**Summary.** “Classically activated macrophages (M1)” and “alternatively activated macrophages (M2)”, which appear in injured tissues, control either inflammation or remodeling. The mechanism remains unclear. To clarify the M1-/M2-macrophage polarization in acute liver injury, M1- and M2-related factors were analysed in F344 rats by a single injection of TAA (300 mg/kg BW), and liver samples were collected on post injection (PI) hour 10 and days 1 to 10. Macrophage immunophenotypes were analyzed by single and double immunolabeling. M1-/M2-related factors were analyzed by real-time RT-PCR. On PI hour 10 (when centrilobular lesions were not still developed), expressions of IFN- $\gamma$ , TNF- $\alpha$ , IL-1 $\beta$ , and IL-6 for M1, and IL-4 for M2 were already increased, followed by increased expressions of IL-10 and TGF- $\beta$ 1 for M2 on PI days 1-3 with development of centrilobular lesions and subsequent reparative fibrosis. On PI hour 10, CD204<sup>+</sup> and MHC class II<sup>+</sup> macrophages already increased in the intact periportal/Glisson’s sheath regions, accompanied by an increased number of granzyme B<sup>+</sup> NK cells. Reactive cells at PI hour 10 might produce M1-related factors. In addition to these macrophages, CD68<sup>+</sup> and CD163<sup>+</sup> macrophages, and CD3<sup>+</sup> T cells appeared in the injured centrilobular region on PI days 1-3; there were macrophages reacting simultaneously to CD68/MHC class II, CD163/MHC class II, CD68/CD204, CD163/CD204, and MHC class

II/CD204 in varying degrees. Although CD68<sup>+</sup> and CD163<sup>+</sup> macrophages are regarded as M1- and M2-types, respectively, the double labeling indicated that macrophage immunophenotypes are interchangeable in injured regions and subsequent fibrosis. An M1-/M2-macrophage paradigm would be useful to analyze hepatotoxicity and to understand the pathogenesis.

**Key words:** Thioacetamide, Liver injury, Macrophage polarization, F344 rats, Immunohistochemistry

## Introduction

Macrophages play important roles in modulating inflammation through phagocytosis, cytokine production, and antigen presentation (Schumann et al., 2000; Yamate et al., 2000). These macrophages may be derived from blood monocytes, histiocytes (Kupffer cells in the liver), and dendritic cells (Gordon and Taylor, 2005). There has been increasing evidence that the more than one type of macrophages appear in inflammation, indicative of the heterogeneity of macrophage population; these macrophages can change their properties depending on microenvironmental conditions (Yamate et al., 2000; Ide et al., 2003; Mori et al., 2009). Resembling the Th1/Th2 nomenclature, macrophages could be named M1- and M2-macrophages; the former are considered to be classically activated macrophages, and the latter are regarded as alternatively activated (or reparative) macrophages (Stein et al., 1992; Martinez et al., 2008). The M1-macrophages appear at the early stages with high tissue damage via production of pro-

*Offprint requests to:* Jyoji Yamate, DVM, PhD, Veterinary Pathology, Division of Veterinary Sciences, Graduate School of Life and Environmental Sciences, Osaka Prefecture University, 1-58, Rinku-ourai-kita, Izumisano city, Osaka. 598-8531. Japan. e-mail: [yamate@vet.osakafu-u.ac.jp](mailto:yamate@vet.osakafu-u.ac.jp)

inflammatory factors, whereas the M2-macrophages resolve inflammatory responses and promote tissue remodeling at the late stages (Gratchev et al., 2001, 2006; Martinez et al., 2008;). M1-macrophages are induced by interferon gamma (IFN- $\gamma$ ) (Martinez et al., 2008). In contrast, interleukin 4 (IL-4) and IL-10 have been found to activate M2-macrophages (Meghari et al., 2007; Martinez et al., 2008; Martinez, 2011).

Hepatic fibrosis is the wound healing in response to hepatocyte injury, leading occasionally to cirrhosis at the advanced stages. The pathogenesis of hepatic fibrosis remains to be clarified in detail. Previously, it was found that macrophages exhibiting various immunophenotypes appear in thioacetamide (TAA)-induced rat hepatic lesions and subsequent fibrosis (Ide et al., 2003; Mori et al., 2009; Wijesundera et al., 2013). Because plasticity and flexibility are key features of macrophages (Sica and Mantovani, 2012), macrophage polarization may have roles in the pathogenesis of toxic-induced hepatic injury and subsequent healing. In the present study, we used an array of macrophage markers (CD68, CD163, MHC class II, and CD204) to detect macrophages with different functions. CD68 is an antigen on lysosomal membranes, and its increased expression implies enhanced phagocytosis (Damoiseaux et al, 1994); CD163 is a scavenger receptor for hemoglobin-haptoglobin complex and its activated expression may be associated with the production of inflammatory factors and phagocytosis (Polfliet et al., 2006); MHC class II molecule is expressed in activated macrophages and dendritic cells (Conrad and Dittel, 2011); CD204 is the scavenger receptor class A, which may be involved in host defense through the ability of phagocytosis and cytokine production, in addition to lipid metabolism (Kiyonagi et al, 2011). To shed some light on the liver pathogenesis, by using these markers we investigated the M1-/M2-macrophage polarization paradigm in TAA-induced acute liver injury in relation to their immunophenotypes and cytokine environment, which is the first attempt for hepatotoxicity analysis.

## Materials and methods

### Animals

Thirty-two 6-week-old male F344 rats (110-120g BW) were obtained from Charles River Japan (Hino,

Shiga, Japan). They were housed in an animal room, maintained at 22 $\pm$ 3°C with a 12 hours light-dark cycle. The animals were fed with a standard diet for rats (DC-8; CLEA, Tokyo, Japan) and provided with tap water *ad libitum*. Twenty-eight rats were given an injection of TAA (Wako Pure Chemical Industries, Osaka, Japan) dissolved in physiological saline (0.9% NaCl) at a dose of 300 mg/kg BW, intraperitoneally. Four rats were euthanized under isoflurane anesthesia on each of post-injection (PI) hour 10, and days 1, 2, 3, 5, 7 and 10. The remaining four rats, which served as controls, received equivalent volumes of physiological saline by intraperitoneal injection and were euthanized on PI hour 10.

Four rats at each examination point were evaluated for each analysis item. Experimental procedures were in agreement with our institutional guidelines on animal care and use, and were conducted in accordance with basic policies for the conduct of animal experimentation of the Ministry of Health, Labor and Welfare Standards relating to the Care and Management of Experimental Animals and the Act on Welfare and Management of Animals, Japan.

### Tissue preparation and histopathology

Livers were removed from all animals. Liver tissues were immediately fixed in 10% neutral buffered formalin or in Zamboni's solution (0.21% picric acid and 2% paraformaldehyde in 130 mM phosphate buffer, pH 7.4). Liver sections were also embedded immediately in Tissu Mount<sup>®</sup> (Chiba Medical Co, Saitama, Japan) and stored at -80°C until further processing. Formalin- and Zamboni's solution-fixed tissues were embedded in paraffin and sectioned at 3-5  $\mu$ m in thickness. Formalin-fixed, de-waxed sections were stained with hematoxyllin and eosin (HE) for histopathological observations and with the azan-Mallory stain for collagen deposition.

### Single immunohistochemistry

Immunohistochemical labeling was performed with peroxidase-conjugated secondary antibody (Histofine simple stain MAX PO<sup>®</sup>; Nichirei Inc., Tokyo, Japan). Zamboni's solution-fixed sections were used for macrophage immunohistochemistry: OX6 (for MHC class II), SRA-E5 (for CD204), ED1 (for CD68), ED2

**Table 1.** Antibodies used in the immunohistochemistry and immunofluorescence.

Immunolabeling antibody to	Antibody type	Fixative	Dilution	Pretreatment	Source
CD68 (ED1)	Mouse monoclonal	Zamboni's	1/1,000	10 $\mu$ g/ml Proteinase K, R/T, 20 min	Millipore, Bedford, Massachusetts, USA
CD163 (ED2)	Mouse monoclonal	Zamboni's	1/500	10 $\mu$ g/ml Proteinase K, R/T, 20 min	AbD Serotec, Oxford, UK
CD204 (SRA-E5)	Mouse monoclonal	Zamboni's	1/500	Microwave in Citrate buffer, 20 min	Transgenic Inc, Kumamoto, Japan
MHC class II (OX6)	Mouse monoclonal	Zamboni's	1/300	Microwave in Citrate buffer, 20 min	AbD Serotec, Oxford, UK
CD3	Rabbit polyclonal	Zamboni's	1/500	Microwave in Citrate buffer, 20 min	Dako Cytomation, Denmark
Granzyme B	Rabbit polyclonal	Zamboni's	1/200	Citrate buffer, 20 min	Spring Bioscience, Pleasanton, CA, USA

MHC, major histocompatibility complex.

## M1-M2-polarization in TAA-treated rat liver

(for CD163). Antibodies against CD3 (for T-lymphocytes) and granzyme B (for NK cells) were also used. Information of primary antibodies used is shown in Table 1. As pre-treatments, sections for MHC class II, CD204, CD3, and granzyme B were boiled in citrate buffer (pH 6) in a microwave for 20 min; for CD68 and CD163, sections were incubated with 10  $\mu$ g/ml proteinase K in 50 mM tris-HCl buffer (pH 7.5) at room temperature for 20 min. Then, all sections were incubated with 5% skimmed milk in phosphate buffered saline (PBS) for 30 min to inhibit nonspecific reactions. These sections were incubated overnight with a primary antibody at 4°C. The sections were treated with 3% H<sub>2</sub>O<sub>2</sub> in PBS for 30 min to quench the endogenous peroxidase activity, followed by the application of secondary antibody for 30 min. Positive reactions were visualized with 3, 3'-diaminobenzidine (DAB; Vector Laboratories Inc., Burlingame, CA, USA). Sections were lightly counterstained with hematoxylin. For negative controls, tissue sections were treated with mouse or rabbit non-immune serum instead of the primary antibodies.

### Double immunofluorescence

Fresh frozen sections (10  $\mu$ m in thickness) were used for double immunofluorescence staining. Sections were fixed in acetone:methanol (1:1) at 4°C for 10 min followed by blocking with 10% normal goat serum in PBS for 30 min at room temperature and incubated with primary antibodies at 4°C overnight. After rinsing with PBS, sections were incubated with goat anti-mouse IgG conjugated to Cy3<sup>®</sup> (Invitrogen, Carlsbad, California, USA; 1 in 1,000) at room temperature for 30 min. For double immunofluorescence with MHC class II, labeled-MHC class II antibody was used. The slides were mounted with SlowFade<sup>®</sup> Gold anti-fade reagent with 4', 6-diamino-2-phenylindole (DAPI; VECTASHIELD<sup>®</sup>; Vector Laboratories, CA, USA) for nuclear stain. Signals were detected and analyzed with a confocal laser scanning microscope system (C1Si; Nikon, Tokyo, Japan).

### Double immunohistochemistry

Because antibodies to CD68, CD163, and CD204 are mouse monoclonal, we could not use the technique of double immunofluorescence. To identify the co-expression of CD204 with CD68 or CD163, therefore, double immunohistochemical staining was performed. Sections were first immunolabeled with CD204 antibody and then visualized with fuchsin substrate-chromogen system (Dako cytomation, Denmark; red in color). Thereafter, the sections were labeled with either CD68 or CD163 and the positive reaction for the second labeling was visualized with DAB (Vector Laboratories Inc., Burlingame, CA, USA; brown in color). To confirm the specificity of the positive reactions, non-immunized mouse serum was used instead of the primary antibodies at each step.

### RNA extraction and real-time quantitative polymerase chain reaction (RT-PCR)

Real-time RT-PCR was performed to evaluate the expression of M1-/M2-macrophage-related factors. Liver samples were immediately soaked in RNA later<sup>®</sup> (Ambion, Texas, USA) and stored at -80°C. Real-time RT-PCR was performed as described previously (Fujisawa et al., 2011). Briefly, total RNA was extracted from liver samples using an SV Total RNA isolation system (Promega, Madison, WI, USA). RNA was reverse-transcribed by using a Superscript VILO<sup>®</sup> reverse transcriptase using random hexamers (Superscript VILO<sup>®</sup>, Invitrogen, Carlsbad, CA, USA). RT-PCR was performed with detection of SYBR green real-time PCR master mix (Toyobo, Osaka, Japan) by a LineGene system (BioFlux, Tokyo, Japan). Primers used are shown in Table 2. The following conditions were used for the amplification: for IFN- $\gamma$ , TNF- $\alpha$ , IL-1 $\beta$ , IL-4, IL-6, and IL-10, 40 cycles of 15 sec of denaturation at 95°C, 15 sec of annealing at 62°C and 20 sec of extension at 72°C; for TGF- $\beta$ 1, 40 cycles of 15 sec of denaturing at 95°C, 15 sec of annealing at 64°C, and 20 sec of extension at 72°C. PCR products were subjected to electrophoresis in 2.5% agarose gel. DNA was stained with ethidium bromide on the gel. Data were calculated using the  $\Delta\Delta$ Ct method. The amount of mRNA was normalized against expression of 18s rRNA as the internal control.

### Cell counts and statistics

Positive cells in sections were counted with NIH imageJ 1.43 freeware (<http://rsbweb.nih.gov/ij/>). CD68<sup>+</sup>, CD163<sup>+</sup>, CD204<sup>+</sup>, MHC class II<sup>+</sup>, CD3<sup>+</sup>, and granzyme B<sup>+</sup> cells were counted per 0.2 mm<sup>2</sup> of tissue in injured

**Table 2.** Primers used in mRNA expression analysis.

Gene name	Sequence
IFN- $\gamma$	(Forward) 5'-TCG CAC CTG ATC ACT AAC TTC TTC-3' (Reverse) 5'-CGA CTC CTT TTC CGC TTC C-3'
TNF- $\alpha$	(Forward) 5'-TGC CTC AGC CTC TTC TCA TTC-3' (Reverse) 5'-GCT CCT CTG CTT GGT GGT TT-3'
IL-1 $\beta$	(Forward) 5'-GCA CCT TCT TTT CCT TCA TCT TTG-3' (Reverse) 5'-TTT GTC GTT GCT TGT CTC TCC TT-3'
IL-6	(Forward) 5'-AAA TGG TCC CCG GAG GT-3' (Reverse) 5'-AAG ACA CAG AGA GAA GCA ATC CAA AC-3'
IL-4	(Forward) 5'-ACC TTG CTG TCA CCC TGT TCT-3' (Reverse) 5'-AGC TCG TTC TCC GTG GTG T-3'
IL-10	(Forward) 5'-CTG TCA TCG ATT TCT CCC CTG T-3' (Reverse) 5'-CAG TAG ATG CCG GGT GGT TC-3'
TGF- $\beta$ 1	(Forward) 5'-CTT CAG CTC CAC AGA GAA CTG C-3' (Reverse) 5'-CAC GAT CAT GTT GGA CAA CTG CTC C-3'
18srRNA	(Forward) 5'-GTA ACC CGT TGA ACC CCA TT-3' (Reverse) 5'-CCA TCC AAT CCG TAG TAG CG-3'

IFN, Interferon; TNF, tissue necrosis factor; IL, Interleukin; TGF, transforming growth factor.

centrilobular regions and periportal regions, including the Glisson's sheath (periportal/Glisson's sheath). The percentage of double-labeled macrophages for CD68<sup>+</sup>/CD204<sup>+</sup>, CD163<sup>+</sup>/CD204<sup>+</sup>, MHC class II<sup>+</sup>/CD204<sup>+</sup>, CD68<sup>+</sup>/MHC class II<sup>+</sup> and CD163<sup>+</sup>/MHC class II<sup>+</sup> were also calculated.

Data obtained in the immunohistochemical analysis and real time RT-PCR experiments were expressed as mean  $\pm$  standard deviation (S.D.). Data were evaluated statistically by the Dunnett's comparison tests, and  $p < 0.05$  was considered significant.

## Results

### TAA-induced acute liver lesions

Control livers showed normal histology (Fig. 1a), and no histopathological lesions were observed in the centrilobular region (Fig. 1b) and periportal/Glisson's sheath regions on PI hour 10. Initial lesions comprising coagulation necrosis of hepatocytes and inflammatory cell infiltration were seen in the centrilobular region on PI day 1 (Fig. 1c). The lesions became more intensive on PI day 2 (Fig. 1d). Inflammatory cells seen in the centrilobular hepatic lesions were mainly macrophages, as demonstrated below by immunohistochemistry. In the injured centrilobular region, fibrosis began to be developed on PI days 2 and 3 (Fig. 1e). The azan-Mallory staining revealed the deposition of collagen fibers in the affected areas with the greatest level on PI day 3 (Fig. 1f). On PI day 5, the fibrotic area with collagen deposition began to be reduced and disappeared completely by PI days 7 and 10, indicative of reparative fibrosis.

### Appearance of various macrophage phenotypes in the injured centrilobular and periportal/Glisson's sheath regions

Macrophages reacting to CD68, CD163, CD204, and MHC class II, and CD3<sup>+</sup> T cells, as well as granzyme B<sup>+</sup> NK cells were evaluated in the centrilobular and periportal/Glisson's sheath regions (Fig. 2).

#### CD68 immunostaining (Fig. 2a)

In control livers, CD68<sup>+</sup> cells were rarely seen in the centrilobular (Fig. 3a) and periportal/Glisson's sheath regions. Following TAA injection, CD68<sup>+</sup> cells were significantly increased on PI days 1 (Fig. 3b) to 3 in the injured centrilobular region, with a peak on day 2 (Fig. 3c). Thereafter, the CD68<sup>+</sup> cell number gradually decreased on day 5, and returned to control level by day 10. In the periportal/Glisson's sheath regions, CD68<sup>+</sup> cells did not show statistically significant changes. The majority of CD68<sup>+</sup> cells were round in shape, and the immunolabeling appeared granular in the cytoplasm (Fig. 3c, inset).

#### CD163 immunostaining (Fig. 2b)

In control sections, CD163<sup>+</sup> cells were observed along sinusoids in the hepatic lobules, indicative of Kupffer cells (Fig. 3d). The CD163<sup>+</sup> cell number showed kinetics similar to that of CD68<sup>+</sup> cells (Figs. 2a and 2b); CD163<sup>+</sup> cells significantly increased in number on PI days 1 (Fig. 3e) to 3, with a peak on PI day 2 (Fig. 3f), and there was no significant change in the periportal/Glisson's sheath regions. The CD163<sup>+</sup> cells were round, spindle or stellate in shape (Fig. 3f, inset).

#### CD204 immunostaining (Fig. 2c)

In control livers, CD204<sup>+</sup> cells were frequently seen along the sinusoids (Fig. 3g), depicting Kupffer cells. In the injured centrilobular regions, CD204<sup>+</sup> cells increased significantly as early as PI hour 10 (Fig. 3h), and the increased number was retained until PI day 2. The maximum number was seen on PI day 1 (Fig. 3i). The CD204<sup>+</sup> cells were spindle or stellate in shape (Fig. 3i, inset). Similarly, the CD204<sup>+</sup> cell number in the periportal/Glisson's sheath regions significantly increased on PI hour 10 to day 2, although the number was less than in the centrilobular region (Fig. 2c).

#### MHC class II immunostaining (Fig. 2d)

Cells reacting to MHC class II were rarely seen in the control liver (Fig. 3j). On PI hour 10, a significantly increased number of MHC class II<sup>+</sup> cells was already seen in the periportal/Glisson's sheath regions (Fig. 3k), although there was no change in the centrilobular regions on PI hour 10. The significantly increased number of MHC class II<sup>+</sup> cells in the periportal/Glisson's sheath regions remained from PI hour 10 to day 3 (Fig. 2d). Furthermore, on PI days 1 to 3, the number of MHC class II<sup>+</sup> cells showed a significantly increase in the injured centrilobular regions (Fig. 2d), with the maximum on PI day 2 (Fig. 3l). The number of MHC class II<sup>+</sup> cells on PI days 1 and 2 was greater in the centrilobular regions than in the periportal/Glisson's sheath regions (Fig. 2d). The majority of MHC class II<sup>+</sup> cells showed large round or polygonal configurations (Fig. 3l, inset).

#### CD3 (Fig. 2e) and granzyme B (Fig. 2f) immunostaining

CD3<sup>+</sup> cells were rarely seen in the hepatic lobules of controls (Fig. 3m). The positive cell number was significantly increased on PI days 1 (Fig. 3n) and 2 in the periportal/Glisson's sheath regions. The number of CD3<sup>+</sup> cells in the injured centrilobular regions showed a transient increase on PI day 2 (Fig. 3o). CD3<sup>+</sup> cells were round or polygonal in shape (Fig. 3o, inset).

In the control livers, there were a few granzyme B<sup>+</sup> cells in the periportal/Glisson's sheath regions (Fig. 3p); however, there were no granzyme B<sup>+</sup> cells in the

## M1-M2-polarization in TAA-treated rat liver

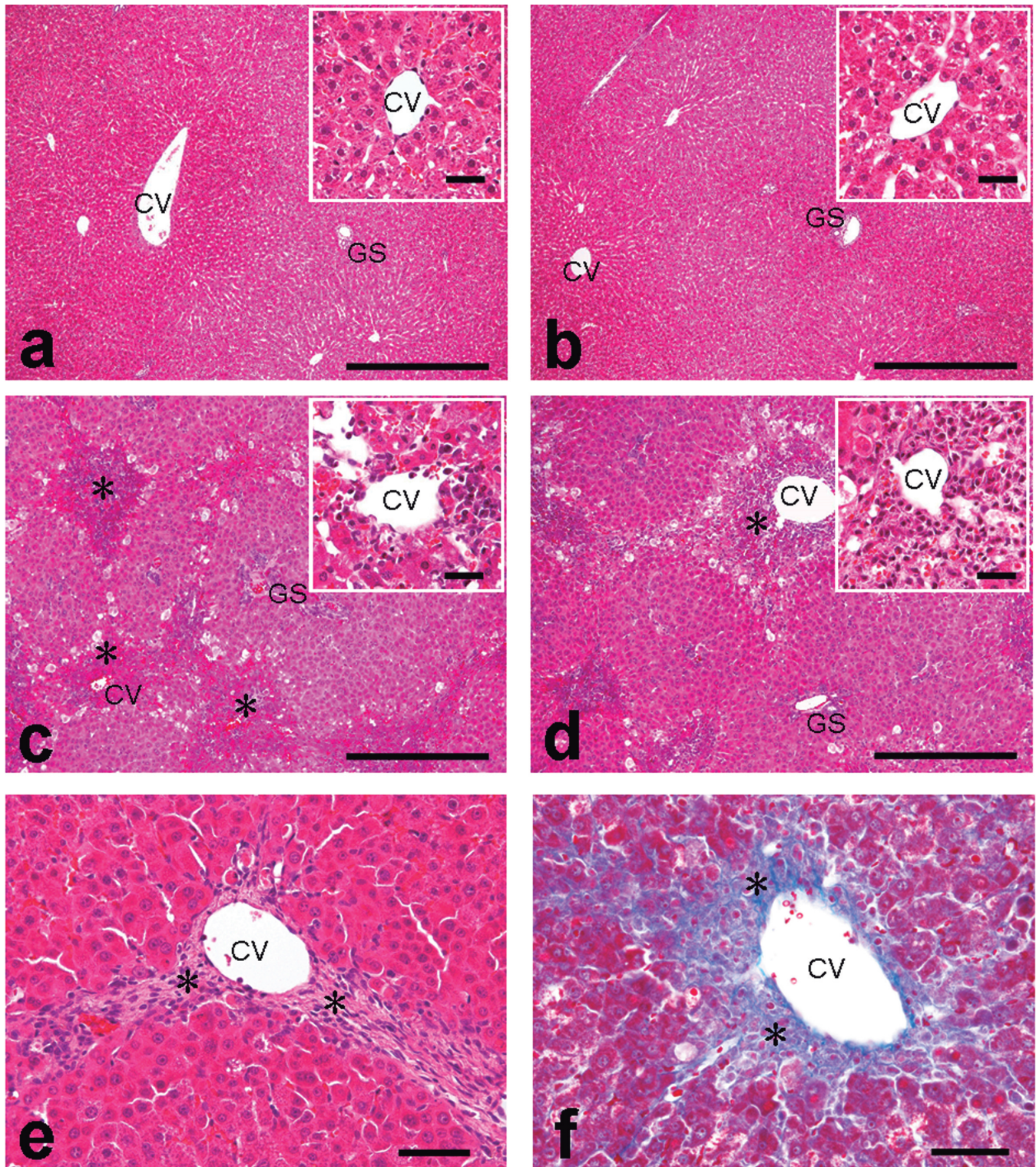


**Fig. 1.** Histopathology of livers of control (a) and thioacetamide (TAA)-injected rats (b-f). Control liver shows normal hepatic architecture (a, inset); no histopathological changes are observed. No histopathological changes are observed in the centrilobular and periportal/Glisson's sheath regions of livers at TAA post-injection (PI) hour 10 (b, inset). Lesions consisting of hepatocyte coagulation necrosis (asterisks) and inflammatory cell reaction is seen in the centrilobular regions on PI day 1 (c, inset). The lesion (asterisk) becomes more intensive in the injured centrilobular regions on PI day 2 (d, inset). Maximum collagen deposition (asterisks) is present in the injured centrilobular regions on PI day 3 (e and f). a-e, HE stain; f, the azan-Mallory stain. CV, central vein; GS, Glisson's sheath. Insets are a higher magnification of each image. bar: 100  $\mu$ m.

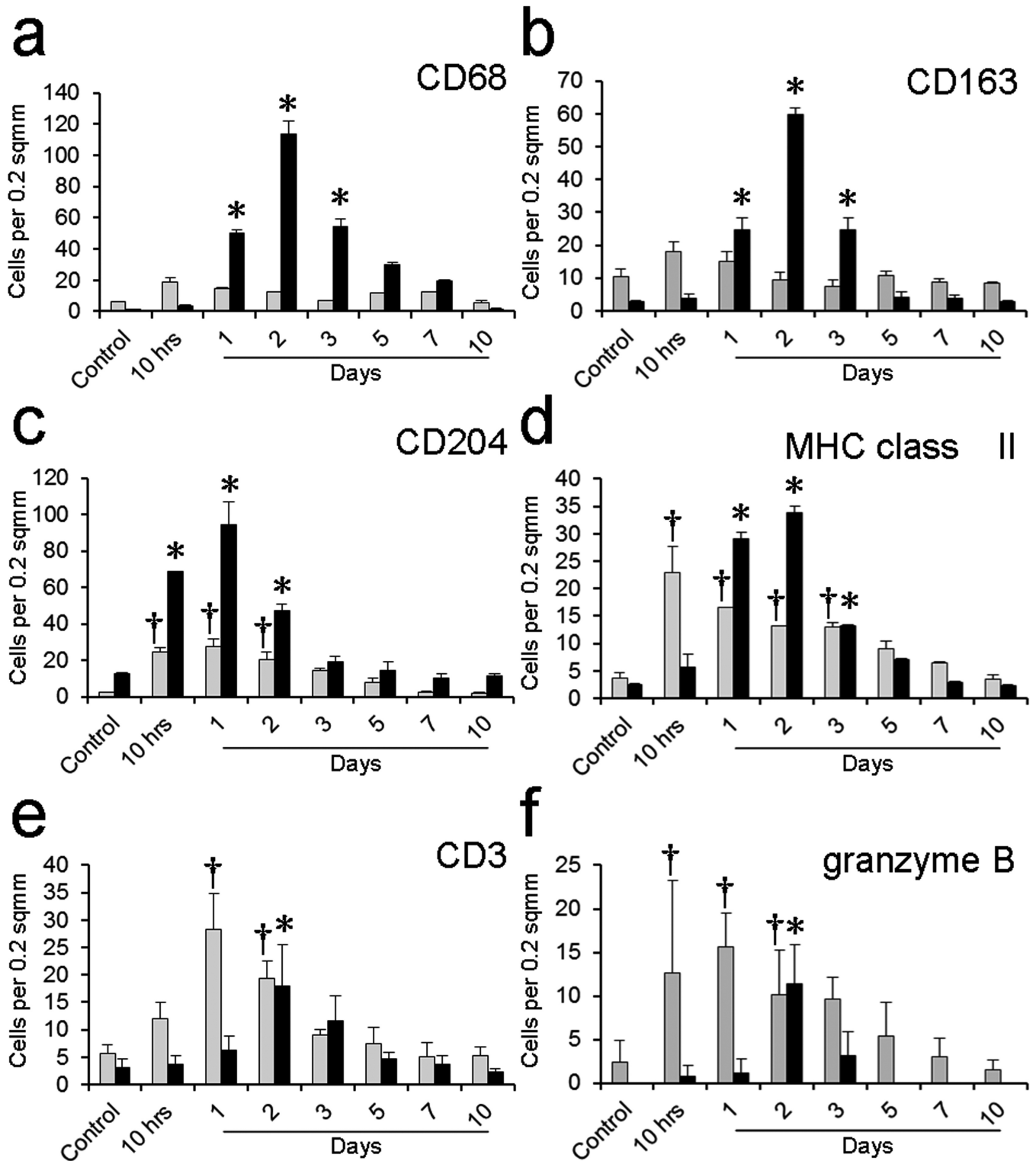


**Fig. 2.** The kinetics of macrophages reacting to CD68 (a), CD163 (b), CD204 (c), MHC class II (d), and CD3<sup>+</sup> T cells (e) and granzyme B<sup>+</sup> NK cells (f) in TAA-induced periportal/Glisson's sheath (grey) or centrilobular (black) regions on hour 10, PI days 1-10 and control. \*, †, significantly different from controls at P<0.05. Bar represents the mean ±S.D.

## M1-M2-polarization in TAA-treated rat liver

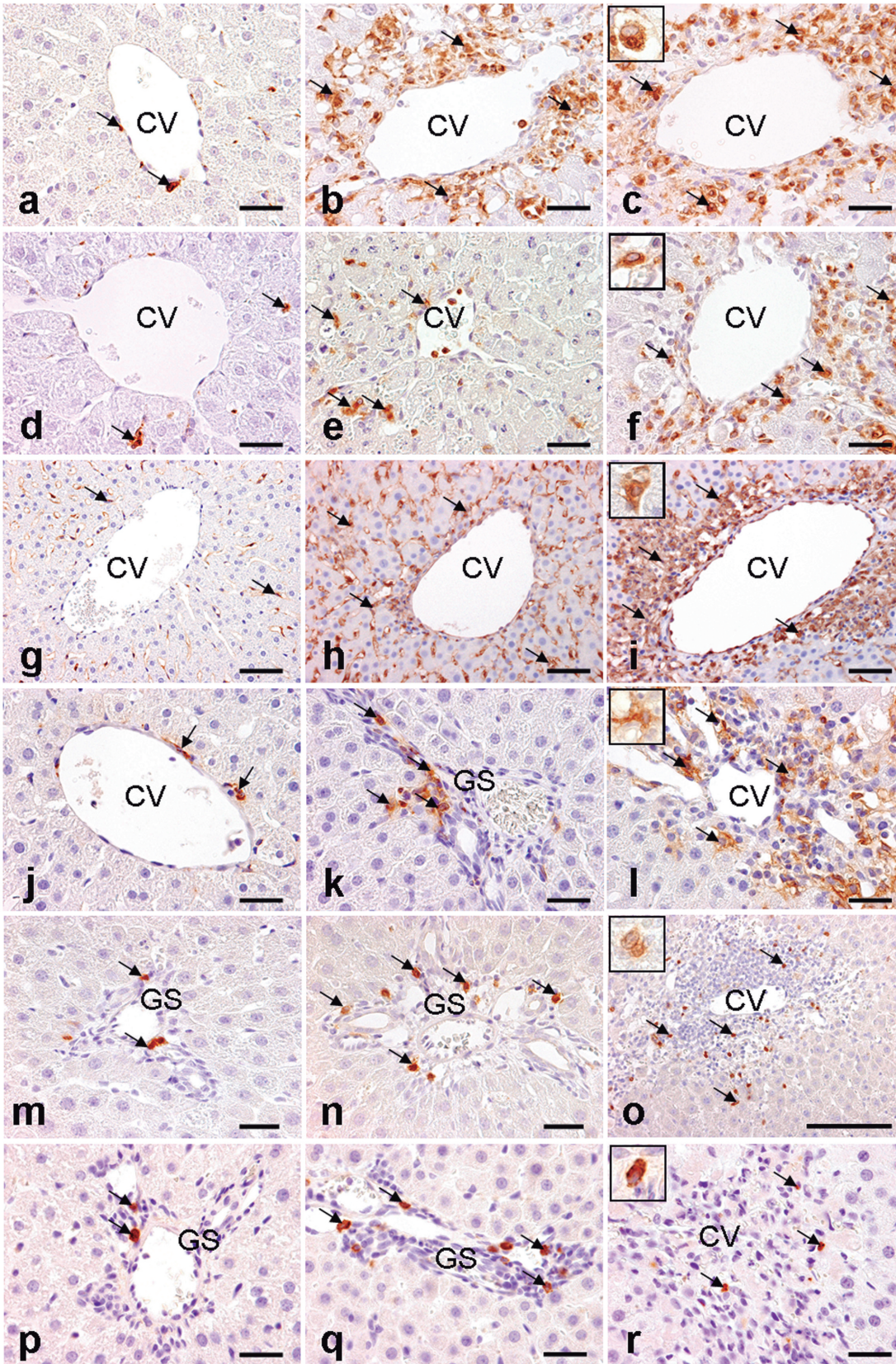


**Fig. 3.** Immunohistochemistry for CD68 (a-c), CD163 (d-f), CD204 (g-i), MHC class II (j-l), CD3 (m-o) and granzyme B (p-r) in control and TAA-treated livers. Macrophages reacting to CD68 (arrows) are rarely seen in the centrilobular region of control liver (a). Many macrophages reacting to CD68 (arrows) are seen in the injured centrilobular region on PI days 1 and 2, respectively (b, c); the positive cells show round morphology, and immune-products appear granular in the cytoplasm (inset). CD163<sup>+</sup> macrophages (arrows) are rarely seen in the control liver (d). Many macrophages reacting to CD163 (arrows) are seen in the injured centrilobular region on PI days 1 and 2 (e, f); the positive cells are round and fusiform in shape (inset). A few CD204<sup>+</sup> macrophages (arrows) are seen in the control liver along the sinusoids depicting Kupffer cells (g). Increased macrophages reacting to CD204 (arrows) are seen in the centrilobular region at PI hour 10 and in the injured centrilobular region on PI day 1 (h, i); the positive cells show large polygonal or spindle shape (inset). MHC class II<sup>+</sup> macrophages (arrows) are rarely seen in the control liver (j). Increased macrophages reacting to MHC class II (arrows) are seen in the Glisson's sheath region on PI hour 10, and in the injured centrilobular region on PI day 2 (k, l); the positive cells are round or polygonal in shape (inset). A few CD3<sup>+</sup> T cells (arrows) are seen in the periportal/Glisson's sheath region in control liver (m). Increased T cells reacting to CD3 (arrows) are seen in the periportal/Glisson's sheath regions on PI day 1 and in the injured centrilobular region on PI day 2 (n, o); CD3<sup>+</sup> T cells are round in shape (inset). A few granzyme B<sup>+</sup> NK cells are seen in the periportal/Glisson's sheath regions in control liver (p). Increased granzyme B<sup>+</sup> NK cells (arrows) are seen in the periportal/Glisson's sheath regions on PI day 1, and in the injured centrilobular region on PI day 2 (q, r); granzyme B<sup>+</sup> cells are round in shape and immunolabeling appears granular in the cytoplasm (inset). Immunohistochemistry, counterstained with hematoxylin. CV, central vein; GS, Glisson's sheath. Bar: 100  $\mu$ m.

1 and in the injured centrilobular region on PI day 2 (n, o); CD3<sup>+</sup> T cells are round in shape (inset). A few granzyme B<sup>+</sup> NK cells are seen in the periportal/Glisson's sheath regions in control liver (p). Increased granzyme B<sup>+</sup> NK cells (arrows) are seen in the periportal/Glisson's sheath regions on PI day 1, and in the injured centrilobular region on PI day 2 (q, r); granzyme B<sup>+</sup> cells are round in shape and immunolabeling appears granular in the cytoplasm (inset). Immunohistochemistry, counterstained with hematoxylin. CV, central vein; GS, Glisson's sheath. Bar: 100  $\mu$ m.

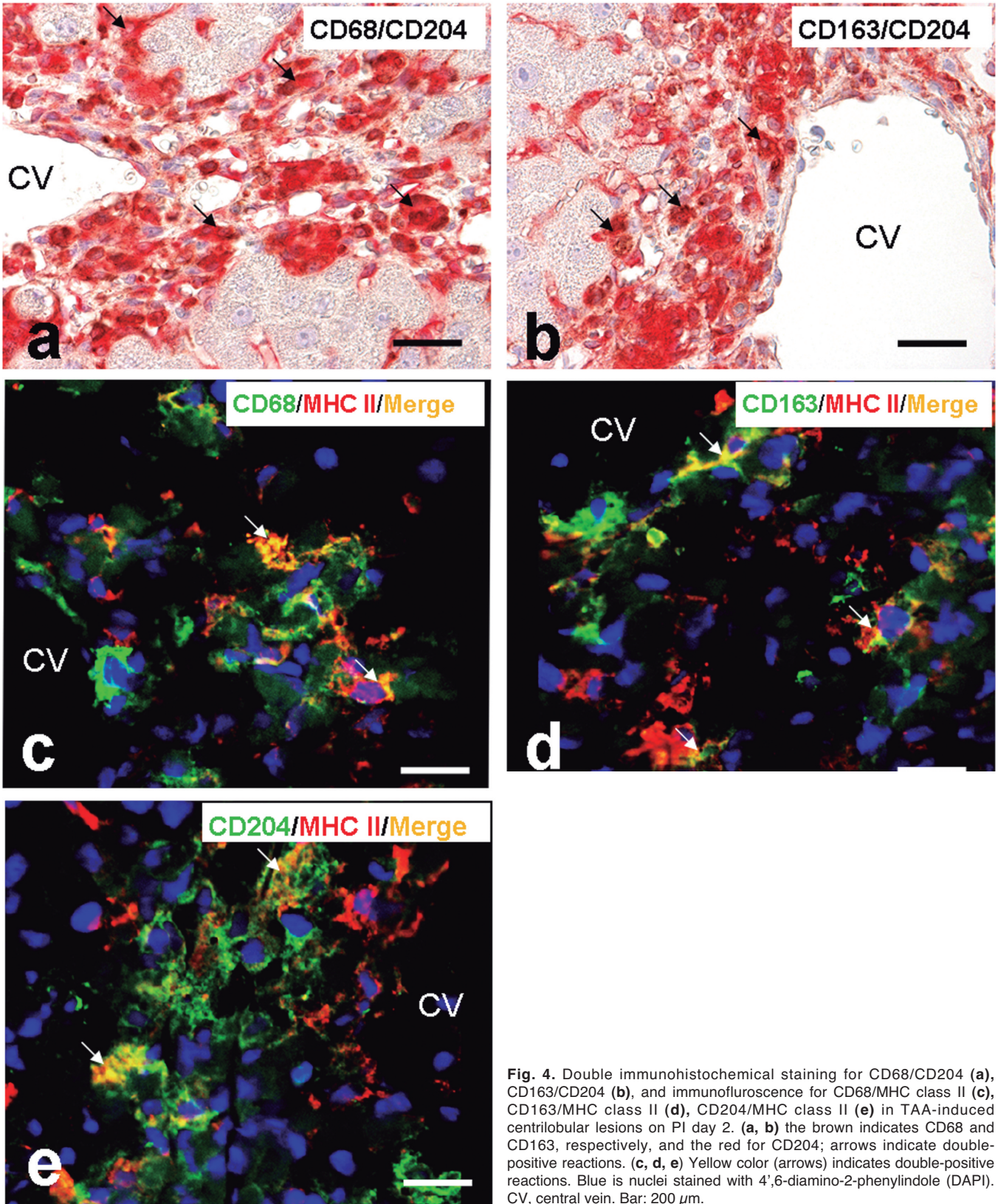


**Fig. 4.** Double immunohistochemical staining for CD68/CD204 (a), CD163/CD204 (b), and immunofluorescence for CD68/MHC class II (c), CD163/MHC class II (d), CD204/MHC class II (e) in TAA-induced centrilobular lesions on PI day 2. (a, b) the brown indicates CD68 and CD163, respectively, and the red for CD204; arrows indicate double-positive reactions. (c, d, e) Yellow color (arrows) indicates double-positive reactions. Blue is nuclei stained with 4',6-diamino-2-phenylindole (DAPI). CV, central vein. Bar: 200  $\mu$ m.

## M1-M2-polarization in TAA-treated rat liver

centrilobular regions. The positive cell number showed a significant increase on PI hour 10 to day 2 in the periportal/Glisson's sheath regions, peaking on day 1 (Fig. 3q). In the injured centrilobular regions, the granzyme B<sup>+</sup> cell number transiently increased on PI day 2 (Fig. 3r). Granzyme B<sup>+</sup> cells were round or polygonal in shape, and immunolabeling appeared granular in the cytoplasm (Fig. 3f, inset). On PI day 3 onwards, the positive cell number both in the centrilobular and periportal/Glisson's sheath regions did not show significant change (Fig. 2f).

### Functional diversity of macrophages in TAA-induced acute liver lesions

To know the different functions of macrophages, double immunolabeling with combinations of CD68/CD204 (Fig. 4a), CD163/CD204 (Fig. 4b), CD68/MHC class II (Fig. 4c), CD163/MHC class II (Fig. 4d), and CD204/MHC class II (Fig. 4e) were conducted in the injured centrilobular regions on PI days 2 and 3. 65% and 20% of MHC class II<sup>+</sup> cells expressed CD68 on PI days 2 and 3 (Fig. 5a), respectively. MHC class II<sup>+</sup> cells reacted to CD163 at the percentages of 35% and 10% on PI days 2 and 3, respectively (Fig. 5b). Expression levels of MHC class II in CD204<sup>+</sup> cells were 67% and 37% on PI days 2 and 3, respectively (Fig. 5c). 55% of CD204<sup>+</sup> cells expressed CD68 on PI day 2 and 38% on PI day 3 (Fig. 5d). CD163 expression in CD204<sup>+</sup> cells was 65% and 95% on PI days 2 and 3, respectively (Fig. 5e). The percentages of cells expressing CD68/MHC class II, CD163/MHC class II, MHC class II/CD204 and CD68/CD204 on PI day 3 showed a significant decrease as compared with those on PI day 2, whereas cells expressing CD163/CD204 on PI day 3 significantly increased the percentage in contrast to that on PI day 2 (Fig. 5).

### Appearance of M1- and M2-related factors in the TAA-induced acute liver lesions

IFN- $\gamma$ , TNF- $\alpha$ , IL-1 $\beta$ , and IL-6 for M1-macrophages and IL-4, IL-10 and TGF- $\beta$ 1 for M2-macrophages were examined (Fig. 6).

mRNAs of IFN- $\gamma$  (Fig. 6a), TNF- $\alpha$  (Fig. 6b), IL-1 $\beta$  (Fig. 6c), and IL-6 (Fig. 6d) showed an abrupt increase as early as PI hour 10 and day 1 and was statistically significant. Except IL-6 mRNA, which remained significantly increased on PI day 2 and began to reduce on PI day 3 (Fig. 6d), the increased mRNA expressions of IFN- $\gamma$ , TNF- $\alpha$ , and IL-1 $\beta$  quickly decreased on PI day 2 and onwards. As compared with controls, mRNA expression for IFN- $\gamma$  (Fig. 6a), TNF- $\alpha$  (Fig. 6b) or IL-1 $\beta$  (Fig. 6c) was approximately 30- and 15-fold greater on PI hour 10 and day 1, respectively. IL-6 mRNA expression showed a 900-fold increase on PI hour 10 and 100-fold increase on PI days 1 and 2 (Fig. 6d).

IL-4 mRNA significantly increased (55-fold) on PI hour 10 (Fig. 6e). mRNA expressions of IL-10 (Fig. 6f)

and TGF- $\beta$ 1 (Fig. 6g) showed a significant increase on PI days 1 to 3, peaking on PI days 1 and 2 for IL-10, and on PI day 3 for TGF- $\beta$ 1. The significant increase on PI days 1-3 was 20- to 30-fold greater for IL-10 (Fig. 6f) and 15- to 40-fold higher for TGF- $\beta$ 1 (Fig. 6g).

## Discussion

### TAA-induced acute liver lesions provide a model to study M1/M2-macrophage polarization

The TAA-induced liver lesion in rats is characterized by coagulation necrosis of hepatocytes and consequent fibrosis in the centrilobular region (Ide et al., 2003; Fujisawa et al., 2011; Wijesundera et al., 2013). Although no histopathological lesions were found on PI hour 10, coagulation necrosis began to be seen in the centrilobular regions on PI day 1, and on PI days 2 and 3, the lesions were more prominent with inflammatory cell reaction (mainly macrophages). In the affected centrilobular regions, fibrosis, demonstrable by the azan-Mallory stain, began to be seen on PI days 2 and 3, with a peak on PI day 3. The fibrotic lesions gradually reduced on PI days 5 and 7, and almost recovered by PI day 10. However, there were no histopathological changes in the periportal/Glisson's sheath regions in TAA-injected rats. These findings bore resemblance to those reported in previous studies (Fujisawa et al., 2011; Wijesundera et al., 2013).

### Macrophages with various immunophenotypes appear differently in the injured centrilobular and periportal/Glisson's sheath regions

Macrophages are an essential component of innate immunity and play a central role in inflammation and host defense (Gordon and Martinez, 2010; Wójcik et al., 2012). To identify reactive macrophages, we used four different antibodies against CD68, CD163, CD204 and MHC class II molecules. Cells reacting to CD68, CD163, and MHC class II showed a significant increase on PI days 1 to 3 in the injured centrilobular regions, peaking on PI day 2; their appearance corresponded to the starting time of development of hepatocyte coagulation necrosis. A similar pattern of CD68<sup>+</sup> and CD163<sup>+</sup> cells has been found in TAA-induced rat liver injury (Wójcik et al., 2012). On the other hand, CD204<sup>+</sup> cells in the centrilobular regions significantly increased as early as PI hour 10 when histopathological changes were not still seen; the CD204<sup>+</sup> cell number peaked on PI day 1, and on PI day 3, they did not show a significant change. More interestingly, on PI hour 10, CD204<sup>+</sup> and MHC class II<sup>+</sup> cells significantly increased in the periportal/Glisson's sheath regions where there were no histopathological lesions throughout the observation period. On PI hour 10, increased CD204<sup>+</sup> cells were along the sinusoids in the periportal regions, whereas MHC class II<sup>+</sup> cells were located exclusively in the Glisson's sheath regions. Taking these findings

together, it was found that macrophages could exhibit divergent immunophenotypes, showing different distribution and kinetics.

*Macrophages show functional diversity in TAA-induced acute liver lesions*

CD163 and CD204 immunohistochemistry label Kupffer cells in normal rat liver (Ide et al., 2003; Golbar

et al., 2012); in fact, cells reacting to CD163 and CD204 were present along the sinusoids of the control livers. On PI hour 10, however, the number of CD204<sup>+</sup> cells both in the centrilobular and periportal/Glisson's sheath regions differed from that of CD163<sup>+</sup> cells, because the former showed a significant increase, whereas the latter did not; these findings indicated that Kupffer cells could display different functions at the pro-inflammatory phases. Because mRNA expressions of IFN- $\gamma$ , TNF- $\alpha$ ,

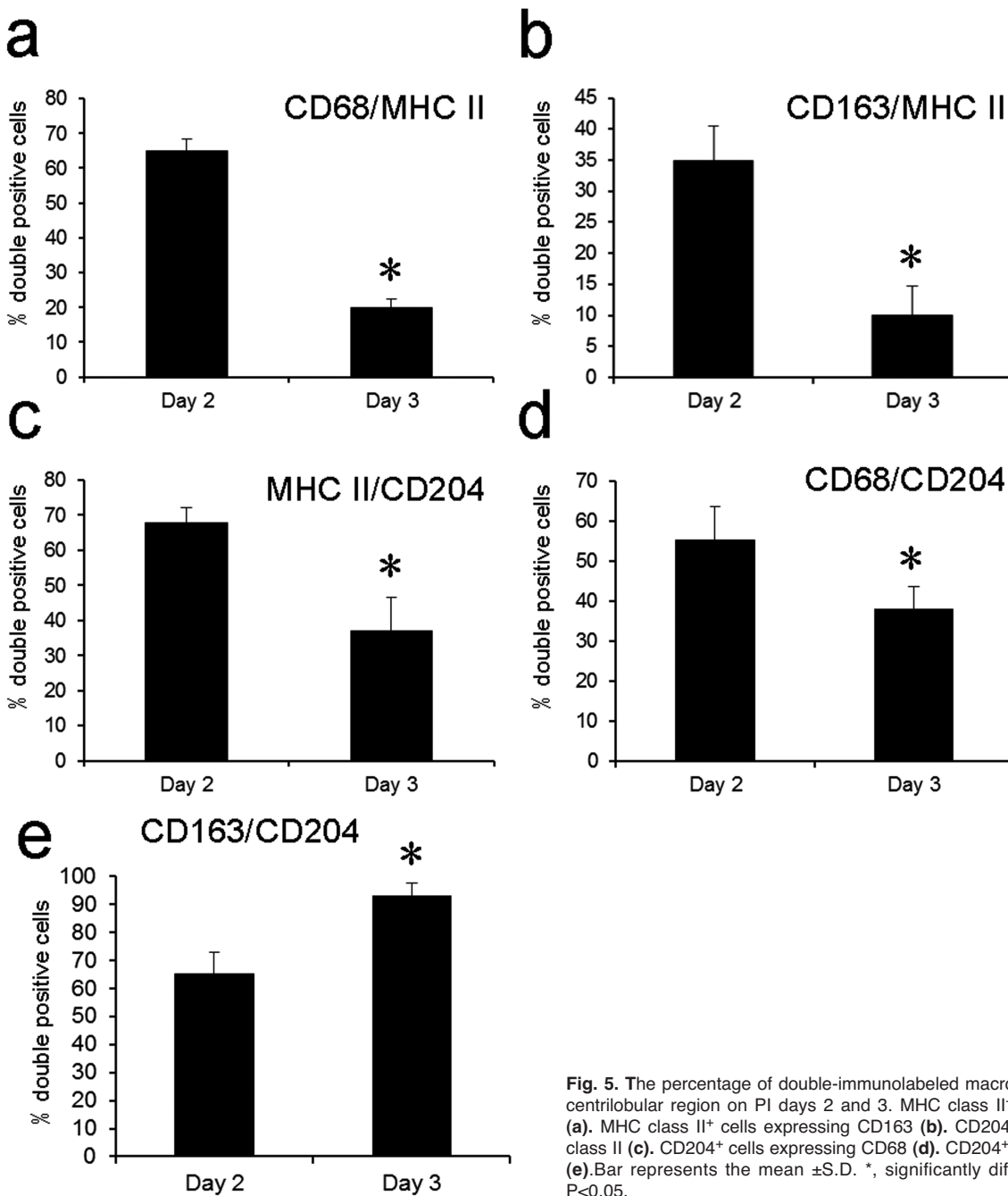


**Fig. 5.** The percentage of double-immunolabeled macrophages in TAA-induced centrilobular region on PI days 2 and 3. MHC class II<sup>+</sup> cells expressing CD68 (a). MHC class II<sup>+</sup> cells expressing CD163 (b). CD204<sup>+</sup> cells expressing MHC class II (c). CD204<sup>+</sup> cells expressing CD68 (d). CD204<sup>+</sup> cells expressing CD163 (e). Bar represents the mean  $\pm$ S.D. \*, significantly different from PI day 2 at P<0.05.

## M1-M2-polarization in TAA-treated rat liver

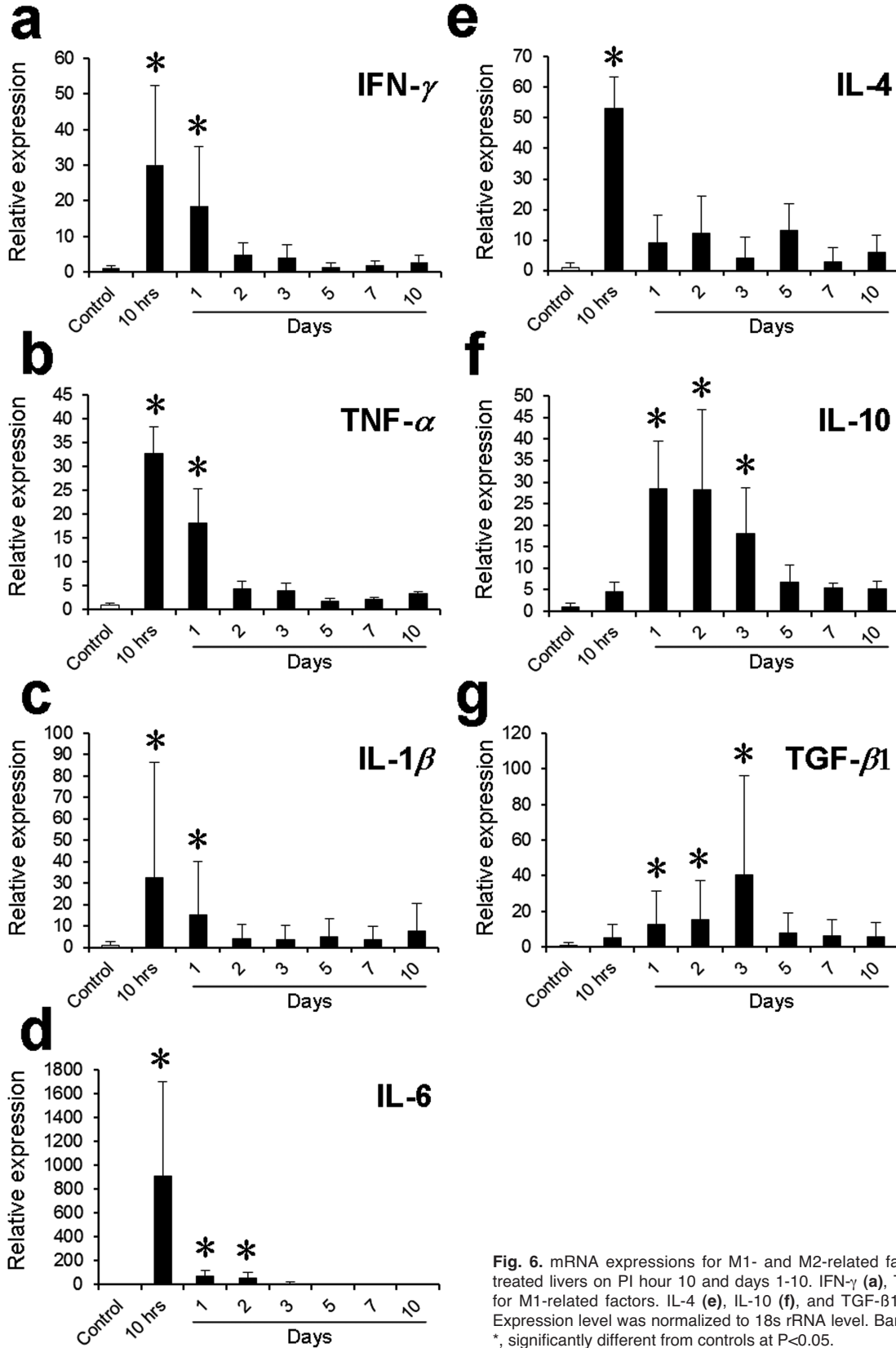


**Fig. 6.** mRNA expressions for M1- and M2-related factors in controls and TAA-treated livers on PI hour 10 and days 1-10. IFN- $\gamma$  (a), TNF- $\alpha$  (b), IL-1, (c), IL-6 (d) for M1-related factors. IL-4 (e), IL-10 (f), and TGF- $\beta$ 1 (g) for M2-related factors. Expression level was normalized to 18s rRNA level. Bar represents the mean  $\pm$ S.D. \*, significantly different from controls at  $P < 0.05$ .

IL-1 $\beta$ , IL-6 and IL-4 significantly increased as early as PI hour 10, CD204<sup>+</sup> Kupffer cells both in the centrilobular and periportal regions might be attributable to such pro-inflammatory factor productions.

Because hepatocyte coagulation necrosis began to be seen on PI days 1 to 3 with inflammatory cell reaction, macrophages reacting to CD68, as well as CD163 and CD204, all of which were seen exclusively in the affected centrilobular regions, would be associated with the phagocytic activity and clearance of necrotic debris. Additionally, because mRNA expression of IL-10 and TGF- $\beta$ 1 significantly increased on PI days 1 to 3, macrophages reacting to CD68, CD163 and CD204 could have produced such factors.

In agreement with the kinetics of CD68<sup>+</sup> and CD163<sup>+</sup> cells, MHC class II<sup>+</sup> cells showed a significant increase on PI days 1 to 3 in the injured centrilobular regions. MHC class II<sup>+</sup> macrophages play a pro-inflammatory role through TNF- $\alpha$  production in diseased brain and kidney (Dietel et al., 2012; Snelgrove et al., 2012). Pre-existing dendritic cells expressing MHC class II also have a pro-inflammatory role in hepatic injury through secretion of TNF- $\alpha$  (Connolly et al., 2009). MHC class II<sup>+</sup> cells might also have responsibility for pro-inflammatory factor production. It is interesting to note that MHC class II<sup>+</sup> cells appeared in the periportal/Glisson's sheath regions with a significant increase on PI hour 10 and the increase remained until PI day 3. Because interstitial dendritic cells are present in the Glisson's sheath (Mori et al., 2009), dendritic cells might be quickly activated in the Glisson's sheath and in the vicinity of the Glisson's sheath.

It is known that MHC class II expression may be related to the activation of T cells and subsequent induction of other macrophages (Perrigou et al., 2009). An increased number of CD3<sup>+</sup> T cells seen in the periportal/Glisson's sheath regions on PI days 1 and 2, and in the centrilobular regions on PI day 2 might be induced by increased MHC class II<sup>+</sup> cells. NK cells can also produce pro-inflammatory cytokines, including IFN- $\gamma$ , TNF- $\alpha$ , IL-4 and IL-10 (Gao et al., 2009; Uemura et al., 2010). Increased CD3<sup>+</sup> T cells and granzyme B<sup>+</sup> NK cells at early stages might be adoptive immunoreactions through MHC class II<sup>+</sup> cells, because both of these lymphocytes increased in the Glisson's sheath regions.

Macrophages can change their properties, such as cytokine production, phagocytosis, and antigen presentation in the inflammatory process (Mosser and Edwards, 2008; Neubauer et al., 2008; Wójcik et al., 2012). Dual immunolabeling analyses conducted on PI days 2 and 3 in the injured centrilobular regions revealed that there were macrophages double-positive to CD68/MHC class II, CD163/MHC class II, MHC class II/CD204, CD68/CD204 or CD163/CD204; on PI day 2, macrophages reacting to CD68/MHC class II, CD163/MHC class II, MHC class II/CD204 and CD68/CD204 were more common, and CD163/CD204-

expressing macrophages were greater in number on PI day 3. These findings indicate that macrophages appearing in the injured hepatic lesions can express some functions in common. It has been reported that monocyte chemoattractant protein-1 (MCP-1) enhances CD68 and CD163 expressions (Mori et al., 2009; Wijesundera et al., 2013), and that TGF- $\beta$ 1 reduces expressions of CD68, CD163, and MHC class II (Kobie et al., 2003). Increased TGF- $\beta$ 1 mRNA expression was seen in the present study, in agreement with increased macrophage populations. Collectively, the properties of macrophages in inflammation are changeable, presumably depending on the microenvironmental factors evoked through cell to cell or cell to matrix interaction.

#### *M1-related factors appear at early stages of acute injury followed by M2-related factors*

According to the concept of M1-/M2-macrophage polarization, IFN- $\gamma$ , TNF- $\alpha$ , IL-1 $\beta$  and IL-6 are possible factors for M1-macrophage induction/activation (Mantovani et al., 2007; Martinez, 2011; Pello et al., 2011). mRNAs of these factors showed a significant increase at very early stages on PI hour 10 and day 1, followed by increased mRNA expressions of IL-10 and TGF- $\beta$ 1 (for M2-macrophage activation) on PI days 1 to 3. Additionally, the present study shows that pro-inflammatory factors such as IFN- $\gamma$ , TNF- $\alpha$ , IL-1 $\beta$  and IL-6 might have been produced by CD204<sup>+</sup> and MHC class II<sup>+</sup> macrophages, as well as granzyme B<sup>+</sup> NK cells, whose the number increased at the early stage in the periportal/Glisson's sheath regions. As discussed above, CD204<sup>+</sup> and MHC class II<sup>+</sup> cells seen on PI hour 10 might be activated Kupffer cells and interstitial dendritic cells, respectively, and the enhanced NK cells (as Pit cells) might be mediated by MHC class II<sup>+</sup> dendritic cells in the Glisson's sheath. The pre-existing macrophages (Kupffer cells and interstitial dendritic cells in the Glisson's sheath), once activated, may play important roles in the induction of M1-macrophages. M1-macrophages can produce superoxide anions, oxygen radicals, and nitrogen radicals under these cytokines, thereby resulting in tissue destruction and host defense (Allavena et al., 2008; Fairweather and Cihakova, 2009). mRNA expression of IL-4, a factor for M2-macrophages (Sica and Mantovani, 2012; Ji et al., 2012), significantly increased as early as PI hour 10, and the increase was transient. The increase timing of IL-4 differed from that of IL-10 and TGF- $\beta$ 1. IL-4 is the major factor for the M2-macrophage induction, whereas expressions of IL-10 and TGF- $\beta$ 1 are regulated by the induced M2-macrophages (Njoku et al., 2009). TGF- $\beta$  may have an antagonizing effect on IFN- $\gamma$  production in macrophages appearing at late stages in hepatotoxicity (Neubauer et al., 2008). Collectively, inflammatory cytokine profiles examined in the present TAA-induced acute rat liver injury might be divided into M1-/M2-macrophage polarization.

### M1-M2-polarization in TAA-treated rat liver

Generally, macrophages expressing CD68 are regarded as the M1-type (Hu et al., 2012; Snelgrove et al., 2012). CD68<sup>+</sup> cells, which significantly increased on PI days 1 to 3 in the injured centrilobular regions, might be induced by IFN- $\gamma$ , TNF- $\alpha$ , IL-1 $\beta$  and IL-6. CD163 is considered as a molecular marker for M2-macrophages, and CD163<sup>+</sup> macrophages have an anti-inflammatory role under regulation of IL-10 and TGF- $\beta$ 1 (Philippidis et al., 2004; Mori et al., 2009; Winnall et al., 2011). We observed an elevation of CD163<sup>+</sup> cell numbers in the injured centrilobular regions on PI days 1 to 3, which agreed with increased expression of IL-10 and TGF- $\beta$ 1 mRNAs. CD163<sup>+</sup> macrophages might play a role in the reparative process as the M2-type; in particular, increased expression of TGF- $\beta$ 1, the major fibrogenic factor (Leask and Abraham, 2004; Meindl-Beinker and Dooley, 2008), can induce myofibroblasts capable of producing collagens leading to fibrosis. In fact, fibrotic lesions began to be seen on PI days 2 and 3 in this study.

M1-macrophages may come to express MHC class II, and facilitate phagocytosis by secreting complement factors (Mantovani et al., 2004). There were CD68<sup>+</sup> macrophages reacting simultaneously to MHC class II on PI days 2 and 3 in the injured centrilobular regions. However, we also observed macrophages reacting both to CD163 and MHC class II. It is likely that MHC class II-expressing dendritic cells seen in the Glisson's sheath on PI hour 10 play roles in the pro-inflammatory response as the M1-type, whereas macrophages reacting to both CD163/MHC class II act as the M2-type in reparative process. Recently, MHC class II-expressing dendritic cells are regarded as M2-macrophages with impaired antigen presentation and increased phagocytic capacity (Soares-Schanoski et al., 2012).

M2-macrophages express high levels of scavenger receptor molecule types A (CD204) and B (Gordon, 2003). The number of CD204<sup>+</sup> cells showed a significant increase on PI hour 10, and days 2 and 3 both in the centrilobular and periportal/Glisson's sheath regions. Additionally, CD204<sup>+</sup> cells on PI days 2 and 3 also gave a positive reaction to MHC class II, CD68 or CD163 in dual immunolabeling. CD204<sup>+</sup> macrophages can function as the M1- or M2-type depending on micro-environmental conditions.

#### *M1-/M2-macrophage transition occurs in TAA-induced acute liver injury*

There is increasing evidence on the interchangeability of M1- and M2- macrophages (Gratchev et al., 2006; Sica et al., 2008; Satoh et al., 2010). Macrophage phenotypes are changed from M1- to M2-types according to tumor progression (Sica et al., 2008), and vice versa in obesity (Satoh et al., 2010). This phenotypic alteration is a result of dedifferentiation of original macrophages back to the resting state or the migration of a new population of macrophages into the tissue site (Gratchev et al., 2006). The present dual immunolabeling showed that there was a possibility of

interchangeability between M1- and M2-macrophages.

In conclusion, the present study shows that M1-/M2-macrophage polarization may be adoptive in TAA-induced acute rat liver lesions. IFN- $\gamma$ , TNF- $\alpha$ , IL-1 $\beta$  and IL-6 for M1-macrophages and IL-4 for M2-macrophages significantly increased at very early stages, followed by increased expressions of IL-10 and TGF- $\beta$ 1 for M2-macrophages at subsequent reparative stages. These M1-macrophage-related factors might be produced by CD204<sup>+</sup> Kupffer cells and MHC class II<sup>+</sup> dendritic cells, as well as granzyme B<sup>+</sup> NK cells present particularly in the periportal/Glisson's sheath regions. Based on the relationship with inflammatory factor profiles, CD68<sup>+</sup> cells are considered to be M1-macrophages, whereas CD163<sup>+</sup> cells are regarded as M2-macrophages. CD68<sup>+</sup> or CD163<sup>+</sup> macrophages also reacted to CD204 and MHC class II, and there were also macrophages positive simultaneously for CD204 and MHC class II in the injured centrilobular regions. There might be a possible transition between M1- and M2-macrophages, indicating the plasticity of macrophages appearing in the hepatic lesions. Human hepatic lesions, which might be caused by various etiologies, show complicated mechanisms induced partly by infiltrating macrophages (Martinez et al., 2008). Although more detailed functions of macrophages should be analyzed, TAA-induced hepatic lesions and subsequent fibrosis would be useful to investigate the hepato-pathogenesis via the M1-/M2-macrophage polarization paradigm.

---

*Acknowledgements.* This work was supported in part by JSPS KAKENHI Grant Numbers 2238017 and 23658265. This work was supported in part by the captioned research programme funded by Food Safety Commission Japan (FSCJ).

---

#### References

- Allavena P., Sica A., Solinas G., Porta C. and Mantovani A. (2008). The inflammatory micro-environment in tumor progression: the role of tumor-associated macrophages. *Crit. Rev. Oncol. Hematol.* 66, 1-9.
- Connolly M.K., Bedrosian A.S., Clair M.S., Mitchell A.P., Ibrahim J., Stroud A., Pachter H.L., Bar-Sagi D., Frey A.B. and Miller G. (2009). In liver fibrosis, dendritic cells govern hepatic inflammation in mice via TNF-alpha. *J. Clin. Invest.* 119, 3213-3225.
- Conrad A.T. and Dittel B.N. (2011). Taming of macrophage and microglial cell activation by microRNA-124. *Cell Res.* 21, 213-216.
- Damoiseaux J.G., Döpp E.A., Calame W., Chao D., MacPherson G.G. and Dijkstra C.D. (1994). Rat macrophage lysosomal membrane antigen recognized by monoclonal antibody ED1. *Immunology.* 83, 140-147.
- Dietel B., Cicha I., Kallmünzer B., Tauchi M., Yilmaz A., Daniel W.G., Schwab S., Garlachs C.D. and Kollmar R. (2012). Suppression of dendritic cell functions contributes to the anti-inflammatory action of granulocyte-colony stimulating factor in experimental stroke. *Exp. Neurol.* 237, 379-387.
- Fairweather D. and Cihakova D. (2009). Alternatively activated macrophages in infection and autoimmunity. *J. Autoimmun.* 33, 222-230.

- Fujisawa K., Miyoshi T., Tonomura Y., Izawa T., Kuwamura M., Torii M. and Yamate J. (2011). Relationship of heat shock protein 25 with reactive macrophages in thioacetamide-induced rat liver injury. *Exp. Toxicol. Pathol.* 63, 599-605.
- Gao B., Radaeva S. and Park O. (2009). Liver natural killer and natural killer T cells: immunobiology and emerging roles in liver diseases. *J. Leukoc. Biol.* 86, 513-528.
- Golbar H.M., Izawa T., Murai F., Kuwamura M. and Yamate J. (2012). Immunohistochemical analyses of the kinetics and distribution of macrophages, hepatic stellate cells and bile duct epithelia in the developing rat liver. *Exp. Toxicol. Pathol.* 64, 1-8.
- Gordon S. and Taylor P.R. (2005). Monocyte and macrophage heterogeneity. *Nat. Rev. Immunol.* 5, 953-964.
- Gordon S. and Martinez F.O. (2010). Alternative activation of macrophages: mechanism and functions. *Immunity* 32, 593-604.
- Gratchev A., Schledzewski K., Guillot P. and Goerdts S. (2001). Alternatively activated antigen-presenting cells: molecular repertoire, immune regulation, and healing. *Skin Pharmacol. Appl. Skin Physiol.* 14, 272-279.
- Gratchev A., Kzhyshkowska J., Köthe K., Muller-Moliniet I., Kannokadan S., Utikal J. and Goerdts S. (2006). Mphi1 and Mphi2 can be re-polarized by Th2 or Th1 cytokines, respectively, and respond to exogenous danger signals. *Immunobiology.* 211, 473-486.
- Hu W., Jiang Z., Zhang Y., Liu Q., Fan J., Luo N., Dong X. and Yu X. (2012). Characterization of infiltrating macrophages in high glucose-induced peritoneal fibrosis in rats. *Mol. Med. Rep.* 6, 93-99.
- Ide M., Yamate J., Machida Y., Nakanishi M., Kuwamura M., Kotani T. and Sawamoto O. (2003). Emergence of different macrophage populations in hepatic fibrosis following thioacetamide-induced acute hepatocyte injury in rats. *J. Com. Pathol.* 128, 41-51.
- Ji Y., Sun S., Xia S., Yang L., Li X. and Qi L. (2012). Short Term High Fat Diet Challenge Promotes Alternative Macrophage Polarization in Adipose Tissue via Natural Killer T Cells and Interleukin-4. *J. Biol. Chem.* 287, 24378-24386.
- Kiyanagi T., Iwabuchi K., Shimada K., Hirose K., Miyazaki T., Sumiyoshi K., Iwahara C., Nakayama H., Masuda H., Mokuno H., Sato S. and Daida H. (2011). Involvement of cholesterol-enriched microdomains in class A scavenger receptor-mediated responses in human macrophages. *Atherosclerosis* 215, 60-69.
- Kobie J.J., Wu R.S., Kurt R.A., Lou S., Adelman M.K., Whitesell L.J., Ramanathapuram L.V., Arteaga C.L. and Akporiaye E.T. (2003). Transforming growth factor beta inhibits the antigen-presenting functions and antitumor activity of dendritic cell vaccines. *Cancer Res.* 63, 1860-1864.
- Leask A. and Abraham D.J. (2004). TGF-beta signaling and the fibrotic response. *FASEB J.* 18, 816-827.
- Mantovani A., Sozzani S., Locati M., Schioppa T., Saccani A., Allavena P. and Sica A. (2004). Infiltration of tumors by macrophages and dendritic cells: tumor-associated macrophages as a paradigm for polarized M2 mononuclear phagocytes. *Novartis Found. Symp.* 256, 137-145.
- Mantovani A., Marchesi F., Porta C., Sica A. and Allavena P. (2007). Inflammation and cancer: breast cancer as a prototype. *Breast* 2, 27-33.
- Martinez F.O. (2011). Regulators of macrophage activation. *Eur. J. Immunol.* 41, 1531-1534.
- Martinez F.O., Sica A., Mantovani A. and Locati M. (2008). Macrophage activation and polarization. *Front. Biosci.* 13, 453-461.
- Meghari S., Berruyer C., Lepidi H., Galland F., Naquet P. and Mege J.L. (2007). Vanin-1 controls granuloma formation and macrophage polarization in *Coxiella burnetti* infection. *Eur. J. Immunol.* 37, 24-32.
- Meindl-Beinker N.M. and Dooley S. (2008). Transforming growth factor-beta and hepatocyte transdifferentiation in liver fibrogenesis. *J. Gastroenterol. Hepatol.* 23, 122-127.
- Mori Y., Izawa T., Takenaka S., Kuwamura M., Yamate J. (2009). Participation of functionally different macrophage populations and monocyte chemoattractant protein-1 in early stages of thioacetamide-induced rat hepatic injury. *Toxicol. Pathol.* 37, 463-473.
- Mosser D.M. and Edwards J.P. (2008). Exploring the full spectrum of macrophage activation. *Nat. Rev. Immunol.* 8, 958-969.
- Neubauer K., Lindhorst A., Tron K., Ramadori G. and Saile B. (2008). Decrease of PECAM-1-gene-expression induced by proinflammatory cytokines IFN- $\gamma$  and IFN- $\alpha$  is reversed by TGF- $\beta$  in sinusoidal endothelial cells and hepatic mononuclear phagocytes. *BMC Physiol.* 8, 9.
- Njoku D.B., Li Z., Washington N.D., Mellerson J.L., Talor M.V., Sharma R. and Rose N.R. (2009). Suppressive and proinflammatory roles for IL-4 in the pathogenesis of experimental DILI. *Eur. J. Immunol.* 39, 1652-1663.
- Pello O.M., Silvestre C., De Pizzol M. and Andrés V. (2011). A glimpse on the phenomenon of macrophage polarization during atherosclerosis. *Immunobiology* 216, 1172-1176.
- Perrigoue J.G., Saenz S.A., Siracusa M.C., Allenspach E.J., Taylor B.C., Giacomini P.R., Nair M.G., Du Y., Zaph C., van Rooijen N., Comeau M.R., Pearce E.J., Laufer T.M. and Artis D. (2009). MHC class II-dependent basophil-CD4<sup>+</sup> T cell interactions promote T(H)2 cytokine-dependent immunity. *Nat. Immunol.* 10, 697-705.
- Philippidis P., Mason J.C., Evans B.J., Nadra I., Taylor K.M., Haskard D.O. and Landis R.C. (2004). Hemoglobin scavenger receptor CD163 mediates interleukin-10 release and heme oxygenase-1 synthesis: anti-inflammatory monocyte-macrophage responses in vitro, in resolving skin blisters in vivo, and after cardiopulmonary bypass surgery. *Circ. Res.* 94, 119-126.
- Polfliet M.M., Fabrick B.O., Daniëls W.P., Dijkstra C.D. and van den Berg T.K. (2006). The rat macrophage scavenger receptor CD163: expression, regulation and role in inflammatory mediator production. *Immunobiology* 211, 419-425.
- Satoh N., Shimatsu A., Himeno A., Sasaki Y., Yamakage H., Yamada K., Suganami T. and Ogawa Y. (2010). Unbalanced M1/M2 phenotype of peripheral blood monocytes in obese diabetic patients: effect of pioglitazone. *Diabetes Care* 33, 7.
- Schumann J., Wolf D., Pahl A., Brune K., Papadopoulos T., van Rooijen N. and Tiegs G. (2000). Importance of Kupffer cells for T-cell dependent liver injury in mice. *Am. J. Pathol.* 157, 1671-1683.
- Sica A. and Mantovani A. (2012). Macrophage plasticity and polarization: in vivo veritas. *J. Clin. Invest.* 122, 787-795.
- Sica A., Larghi P., Mancino A., Rubino L., Porta C., Totaro M.G., Rimoldi M., Biswas S.K., Allavena P. and Mantovani A. (2008). Macrophage polarization in tumour progression. *Semin. Cancer Biol.* 18, 349-355.
- Snelgrove S.L., Kausman J.Y., Lo C., Lo C., Ooi J.D., Coates P.T., Hickey M.J., Holdsworth S.R., Kurts C., Engel D.R. and Kitching A.R. (2012). Renal dendritic cells adopt a pro-inflammatory phenotype in obstructive uropathy to activate T cells but do not directly contribute to fibrosis. *Am. J. Pathol.* 180, 91-103.

*M1-M2-polarization in TAA-treated rat liver*

- Soares-Schanoski A., Jurado T., Córdoba R., Silíceo M., Fresno C.D., Gómez-Piña V., Toledano V., Vallejo-Cremades M.T., Alfonso-Iñiguez S., Carballo-Palos A., Fernández-Ruiz I., Cubillas-Zapata C., Biswas S.K., Arnalich F., García-Río F. and López-Collazo E. (2012). Impaired antigen presentation and potent phagocytic activity identifying tumor-tolerant human monocytes. *Biochem. Biophys. Res. Commun.* 423, 331-337.
- Stein M., Keshav S., Harris N. and Gordon S. (1992). Interleukin 4 potently enhances murine macrophage mannose receptor activity: a marker of alternative immunologic macrophage activation. *J. Exp. Med.* 176, 287-292.
- Uemura A., Takehara T., Miyagi T., Suzuki T., Tatsumi T., Ohkawa K., Kanto T., Hiramatsu N. and Hayashi N. (2010). Natural killer cell is a major producer of interferon gamma that is critical for the IL-12-induced anti-tumor effect in mice. *Cancer Immunol. Immunother.* 59, 453-463.
- Wijesundera K.K., Juniantito V., Golbar H.M., Fujisawa K., Tanaka M., Ichikawa C., Izawa T., Kuwamura M. and Yamate J. (2013). Expression of Iba1 and galectin-3 (Gal-3) in thioacetamide (TAA)-induced acute rat liver lesions. *Exp. Toxicol. Pathol.* 65, 799-808.
- Winnall W.R., Muir J.A. and Hedger M.P. (2011). Rat resident testicular macrophages have an alternatively activated phenotype and constitutively produce interleukin-10 in vitro. *J. Leukoc. Biol.* 90, 133-143.
- Wójcik M., Ramadori P., Blaschke M., Sultan S., Khan S., Malik I.A., Naz N., Martius G., Ramadori G. and Schultze F.C. (2012). Immunodetection of cyclooxygenase-2 (COX-2) is restricted to tissue macrophages in normal rat liver and to recruited mononuclear phagocytes in liver injury and cholangiocarcinoma. *Histochem. Cell Biol.* 137, 217-233.
- Yamate J., Yoshida H., Tsukamoto Y., Ide M., Kuwamura M., Ohashi F., Miyamoto T., Kotani T., Sakuma S. and Takeya M. (2000). Distribution of cells immunopositive for AM-3K, a novel monoclonal antibody recognizing human macrophages, in normal and diseased tissues of dogs, cats, horses, cattle, pigs, and rabbits. *Vet. Pathol.* 37, 168-176.

Accepted October 11, 2013